Cascading implementation of a magnetocaloric heat pump for building space heating applications

Johra, Hicham; Filonenko, Konstantin; Heiselberg, Per; Veje, C.; Dall'Olio, Stefano ; Engelbrecht, Kurt; Bahl, Christian

Cascading implementation of a magnetocaloric heat pump for building space heating applications

H. Johra[1]*, K. Filonenko[2], P. Heiselberg[1], C. Veje[2], S. Dall'Olio[3], K. Engelbrecht[3], C. Bahl[3]

(1) Aalborg University, Division of Architectural Engineering, Department of Civil Engineering

Thomas Manns Vej 23, DK-9220 Aalborg Øst, Denmark

(2) University of Southern Denmark, Center for Energy Informatics

Campusvej 55, DK-5230 Odense M, Denmark

(3) Technical University of Denmark, Department of Energy Conversion and Storage

Frederiksborgvej 399, DK-4000 Roskilde, Denmark

ABSTRACT

The main objective of the ENOVHEAT project is to develop, build and test the prototype of an innovative and efficient heat pump system based on the active magnetic regenerator technology and to demonstrate that it can be used for building space heating applications. The numerical investigation presented in this article tested different configurations of single magnetocaloric heating systems and cascaded magnetocaloric heating networks. It has been shown that the magnetocaloric heat pump can provide for the heating need of a single family house under Danish winter weather condition and presents appreciable coefficient of performance. At optimum fluid flow rate, certain magnetocaloric heat pump configurations could generate fluid temperature outlet of up to 35.3 °C and COPs of up to 4.45. When integrated and operating in a multi-zone dwelling, magnetocaloric heat pump presented average seasonal COPs of up to 1.84 and 2.63 for single unit systems and cascaded magnetocaloric heating networks, respectively. These results are encouraging to continue investigating further the magnetocaloric heat pump technology.

Keywords: Magnetocaloric heat pump, magnetic heating, active magnetic regenerator, innovative heating system, cascading configuration.

1. INTRODUCTION

To tackle the problems of CO_2 emissions and pollution, mitigate the effects of climate change, and meet crucial energy and environmental goals, our modern industrial societies must operate a transition towards decarbonized and renewable energy sources. However, a global decrease of our energy usage is also necessary, which implies a sharp efficiency improvement of the different energy systems.

The building sector has clearly been identified as the main target for energy savings as it is the largest energy end-user in the world. In Europe, for example, the buildings represent 40% of the total energy demand, among which 75% is used for indoor space heating (BPIE, 2011). A large share of this heating need can be cut down by enhancing the thermal performance of the building's envelope and improving the energy efficiency of the heating systems (IEA, 2013). In regards to the latter, heat pumps were found to be an excellent cost-effective heating supply helping to establish a sustainable building stock with low greenhouse gas emissions, and facilitating the integration of a large share of renewable energy sources (Cockroft and

Kelly, 2006; Lund et al., 2010; Palzer and Henning, 2014). Consequently, heat pump systems became a key component of the energy development planning of many countries and their market has shown continuous growth over the last decade.

Currently, the heat pump market is dominated by conventional systems based on a vapour-compression thermodynamic cycle to transfer heat from a cold reservoir (heat source) to a hot reservoir (heat sink). This mature technology has proved its cost-effectiveness in industrial and building applications with high coefficient of performance (COP), typically ranging from 3 to 5 (Self et al., 2013; Fischer and Madani, 2017).

Promising alternatives to conventional vapour-compression heat pumps are devices based on the active magnetic regenerator (AMR) cycle employing the magnetocaloric effect (MCE). Because of the reversible nature of the MCE, AMR-based systems have a great potential for high COP. Moreover, they can operate with low vibration and noise level, have the possibility of recycling their components, and do not employ any toxic or greenhouse gases (Smith et al., 2012). The latest magnetocaloric prototypes developed by different research team present encouraging performance for cooling applications. The rotary AMR device of Engelbrecht et al. (2012) has a cooling capacity of 1010 W and a 25.4 K no-load temperature span. The magnetic cooling machine of Okamura and Hirano (2013) was operating at a COP of 2.5 with a 5 K temperature span. Jacobs et al. (2014) reported a prototype with 2502 W of cooling power at a COP above 2 and a temperature span of 12 K. The magnetocaloric device of Eriksen et al. (2016) has a cooling power of 81.5 W with a COP of 3.6 and a temperature span of 15.5 K.

The ENOVHEAT project (Bahl, 2015) aims at demonstrating that AMR-based systems can be integrated in buildings as a magnetocaloric heat pump (MCHP) and be able to provide for the indoor space heating needs. A previous publication from Johra et al. (2018) has presented a numerical study showing that the MCHP of the ENOVHEAT project can be integrated in a low-energy single family house under Danish winter weather conditions. However, the limited temperature span of this MCHP prototype restricts its application to low-temperature under-floor heating system for well-insulated buildings.

The objective of this article is to present the results of a numerical investigation testing innovative cascading implementations of AMR systems in order to increase the MCHP temperature span and provide for the indoor space heating of poorly-insulated buildings. Firstly, the operational principle and characteristics of the MCHP prototype are described. Details about the building study case and numerical models are then presented. The performances of two types of MCHP with and without cascading implementation are then compared in the case of poorly-insulated and well insulated buildings. Finally, a conclusion and suggestions for further research close this article.

2. THE MAGNETOCALORIC HEAT PUMP

2.1 The magnetocaloric effect and the active magnetic regenerator cycle

The magnetocaloric effect is a reversible temperature change that occurs in a magnetocaloric material (MCM) when subjected to an adiabatic magnetization or demagnetization. When a magnetic field is applied to the MCM, its magnetic entropy decreases and, consequently, its temperature increases. Reciprocally, when the MCM is demagnetized, its magnetic entropy increases and its temperature decreases (Smith et al., 2012).

The magnetocaloric effect was discovered a century ago by Weiss and Piccard (1918). At first, the MCE was only used for laboratory cooling purposes at absolute temperatures below 1 K (Giauque and MacDougall, 1935).

In 1982, Barclay and Steyert (1982) developed the active magnetic regenerator cycle (see *Figure 1*) which employs the MCM as a thermal regenerator. It allows to generate temperature spans which are much larger than the adiabatic temperature change of the MCE alone. The solid refrigerant MCM is contained as a porous media in a regenerator which is alternatively magnetized and demagnetized with an external magnetic field source (e.g., a rotating permanent magnet). The bi-directional circulation of a coolant fluid through the MCM exhibiting a magnetocaloric response performs the heat transfer from a heat source (cold side) to a heat sink (hot side) (Johra, 2018). The AMR technology is considered to be the most thermodynamically efficient principle for magnetocaloric heat pumps (Chen et al., 1992). AMR-based devices are therefore the most common MCHP systems for near room-temperature magnetic heating and cooling applications.

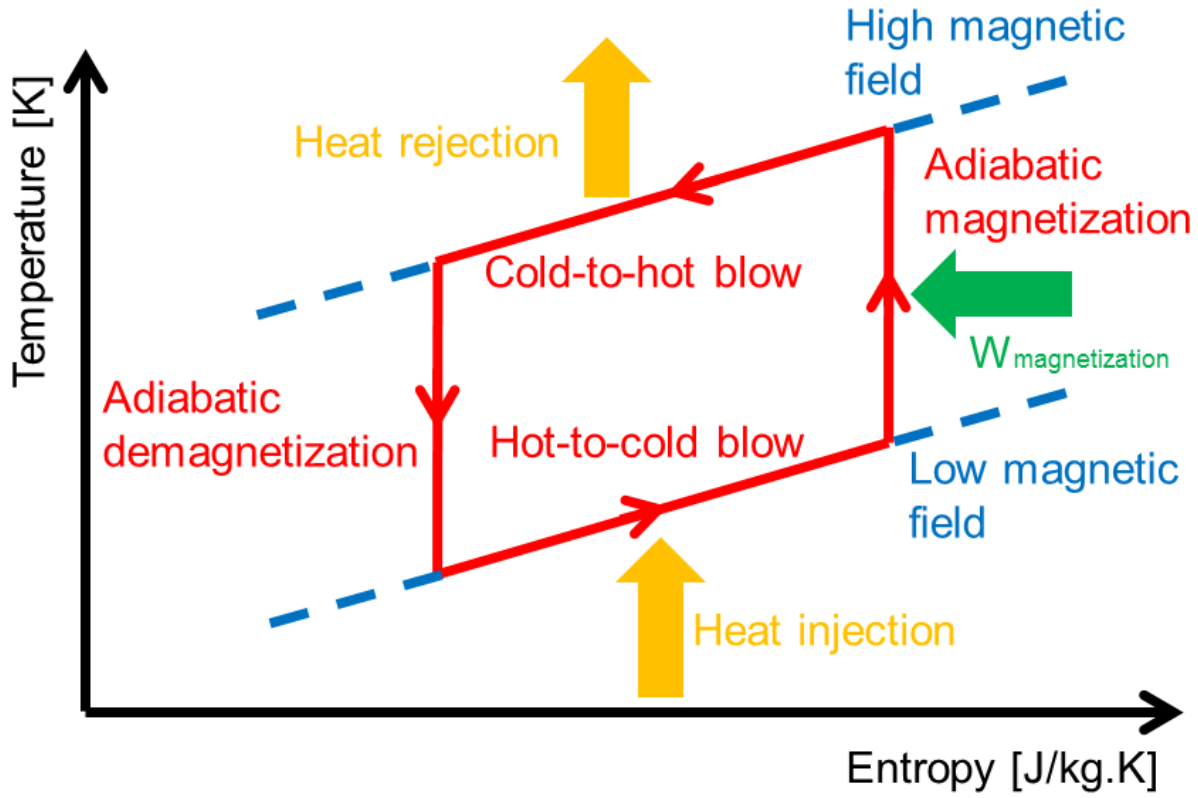

Figure 1: Temperature–entropy diagram of the AMR cycle (Johra, 2018).

Gadolinium (Gd) is considered to be the reference material for MCE at near room-temperature (Smith et al., 2012). As an alternative to this rare earth element, intermetallic compounds such as $La(Fe,Mn,Si)_{13}H_y$ have shown very interesting magnetocaloric properties. These compounds can also exhibit a large MCE at near-room-temperature but are composed of chemical elements which are more abundant and low-cost than Gadolinium (Smith et al., 2012). In addition, the Curie temperature of these MCMs can be adjusted precisely to optimize the MCE inside the AMR (graded or multi-layered regenerator) according to the inherent temperature gradient inside the latter (Navickaitė et al., 2018).

Extensive explanations of the magnetocaloric effect and active magnetic regenerator devices can be found in Smith et al. (2012), Kitanovski et al. (2015) and Engelbrecth et al. (2012).

2.2 Characteristics of the magnetocaloric heat pump

The MCHP prototype developed by the ENOVHEAT project and currently under testing at the Technical University of Denmark (DTU) is a rotary AMR system (see *Figure 2*). 13 active magnetic regenerators mounted on an iron ring compose the vertical stator. The vertical rotor is composed of a two-pole magnet assembly attached to a shaft which is driven by an electrical motor. The rotation of the magnets (rotation frequency ranging from 0.5 Hz to 4 Hz) creates a varying magnetic field (maximum value of 1.46 Tesla) in the regenerators which alternately magnetizes and demagnetizes the MCM. The 13 AMRs are connected to 2 manifold collectors and 2 manifold distributors, one of each for the heat source and similarly for the heat sink. 26 synchronized valves control the bi-directional flow of the heat transfer fluid (20%vol ethylene glycol; 80%vol water) through the individual regenerators (Johra et al., 2018).

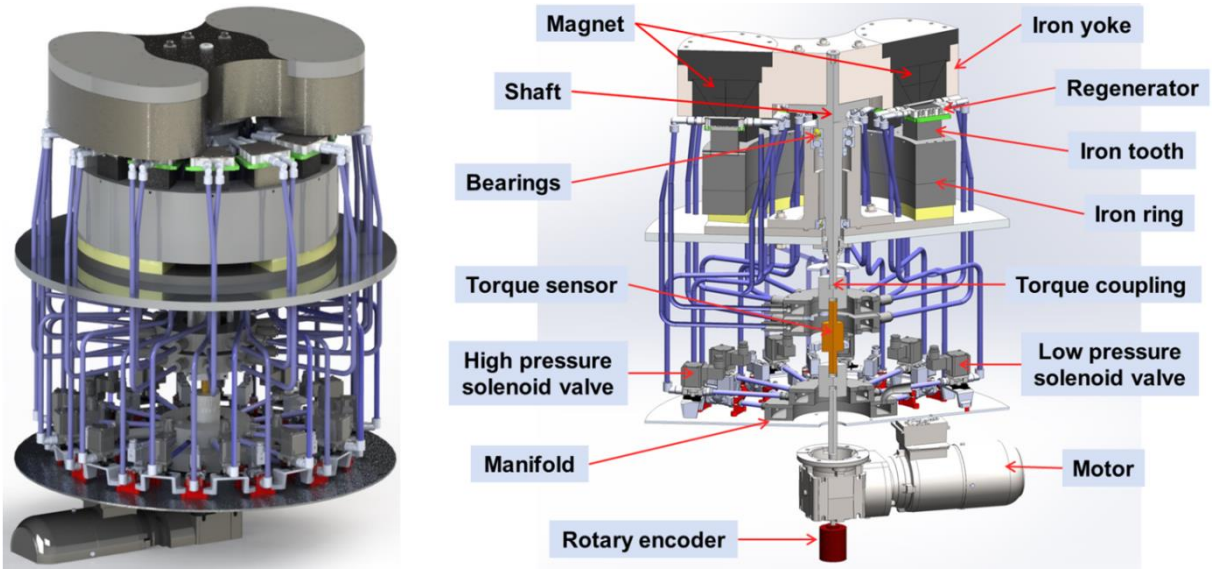

Figure 2: Full view CAD model (left) and detailed description (right) of the magnetocaloric heat pump prototype of the ENOVHEAT project: "MagQueen".

The magnetocaloric material is placed inside the trapezoidal shaped-cassette regenerators as packed bed spheres. In the current numerical investigation, two types of MCM are tested: Gadolinium and $La(Fe,Mn,Si)_{13}H_y$. In the case of $La(Fe,Mn,Si)_{13}H_y$, the Curie temperature of the MCM is adjusted so that 10 layers in the AMR are formed with optimized operational temperatures for maximizing the MCE.

2.3 Modelling of the magnetocaloric heat pump

The original detailed numerical model of the AMR prototype was created by Engelbrecht (2008), then further developed by Lei et al. (2017), and validated with experimental data of different AMR prototypes. With reasonable assumptions on regenerator's geometry, external heat losses and demagnetization losses, the time-dependent fluid temperature distribution in the AMR can be calculated with the two following coupled partial differential equations:

$$\frac{\partial}{\partial x}\left(k_{\mathrm{disp}}A_{\mathrm{c}}\frac{\partial T_f}{\partial x}\right)-\dot{m}_f c_f\frac{\partial T_f}{\partial x}-\frac{Nuk_f}{d_h}a_s A_{\mathrm{c}}\left(T_f-T_s\right)+\left|\frac{\partial P}{\partial x}\frac{\dot{m}_f}{\rho_f}\right|=A_{\mathrm{c}}\varepsilon\rho_f c_f\frac{\partial T_f}{\partial t} \quad (1)$$

$$\frac{\partial}{\partial x}\left(k_{\text{stat}} A_c \frac{\partial T_s}{\partial x}\right) + \frac{\text{Nu} k_f}{d_h} a_s A_c \left(T_f - T_s\right) = A_c \left(1-\varepsilon\right) \rho_s \times \left[c_H \frac{\partial T_s}{\partial t} + T_s \left(\frac{\partial s_s}{\partial H}\right)_{T_s} \frac{\partial H}{\partial t} \right] \quad (2)$$

Where k, T, ρ, c and s are the thermal conductivity, temperature, density, specific heat, and specific entropy; A_c, d_h, a_s, ε, x, t, $\dot{m}_f$, and H are the cross sectional area, hydraulic diameter, specific surface area, porosity of the regenerator bed, axial position, time, fluid mass flow rate and internal magnetic field; $\partial P / \partial x$ and Nu are the pressure drop and the Nusselt number. The subscripts f and s represent fluid and solid refrigerant, respectively. k_{disp} is the thermal conductivity of the fluid due to axial dispersion, k_{stat} is the static thermal conductivity of regenerator and fluid, and c_H is the specific heat capacity of the MCM at constant magnetic field.

These partial differential equations are originally solved with an implicit finite volume method scheme. However, this detailed model is too computationally demanding for a direct use in a building simulation tool. It is therefore approximated by 5-dimentional interpolation lookup table functions containing around 1600 output points generated by the detailed model with the parameters of the ENOVHEAT MCHP prototype.

The other components of the MCHP (valves, motor, circulation pump) are modelled with simple functions fitting data from measurements on the prototype and from manufacturers documentation (Johra et al., 2018).

3. THE BUILDING SYSTEM

3.1 Building study cases

Two versions of the same building with different envelope thermal performances are chosen for testing the MCHP configurations. The building study cases are based on a typical Danish single-story single family house (4 occupants) with 126 m² of heated floor surface area. One house is a well-insulated building with a yearly heating need of 16 kWh/m². The other house is a poorly-insulated building with a yearly heating need of 160 kWh/m². The dwellings are equipped with a hydronic radiant under-floor heating (UFH) system which is the heat sink of the MCHP. In the case of the well-insulated dwelling, the heat source of the heating system is a single collector vertical borehole ground source heat exchanger (VBGSHE) with a depth of 100 m. For the poorly-insulated house, the heat source consists of two VBGSHE of 100 m depth each. The outdoor boundary conditions are extracted from weather file of the national Danish Reference Year 2013 (Johra, 2018).

3.2 Building modelling

Thermodynamic multi-zone models of the building study cases have been created within the MATLAB-Simulink software environment. The heat transfer through the different planar construction elements is calculated with a one-dimensional finite volume method formulation comprising a limited number of control volumes (also known as Resistance-Capacitance or RC thermal network model). Each building model has 10 thermal zones. The UFH system and the VBGSHE are modelled by coupling a “plug flow” model with the ε-NTU method which accounts for the thermal interactions between the adjacent legs of the hydronic circuits. The simulation time step size is set constant to 60 seconds which ensures numerical stability. The entire building model and its sub-components have been validated against well-known

commercial software (BSim and COMSOL Multiphysics), experimental data, and with a BESTEST procedure (Johra, 2018).

4. INTEGRATION OF THE MAGNETOCALORIC HEAT PUMP IN BUILDINGS

4.1 Single hydronic loop implementation

The different MCHP configurations can operate at temperatures and fluid flow rates which are compatible with a direct use in the UFH emitters. The MCHP is therefore integrated in the building heating system within a single hydronic loop connecting the VBGSHE and the UFH circuits (see *Figure 3*). There is no intermediate heat exchanger or water storage tank in the circuit and the same heat transfer fluid is circulated through the VBGSHE, the UFH and the MCHP by a single circulation pump (Johra, 2018).

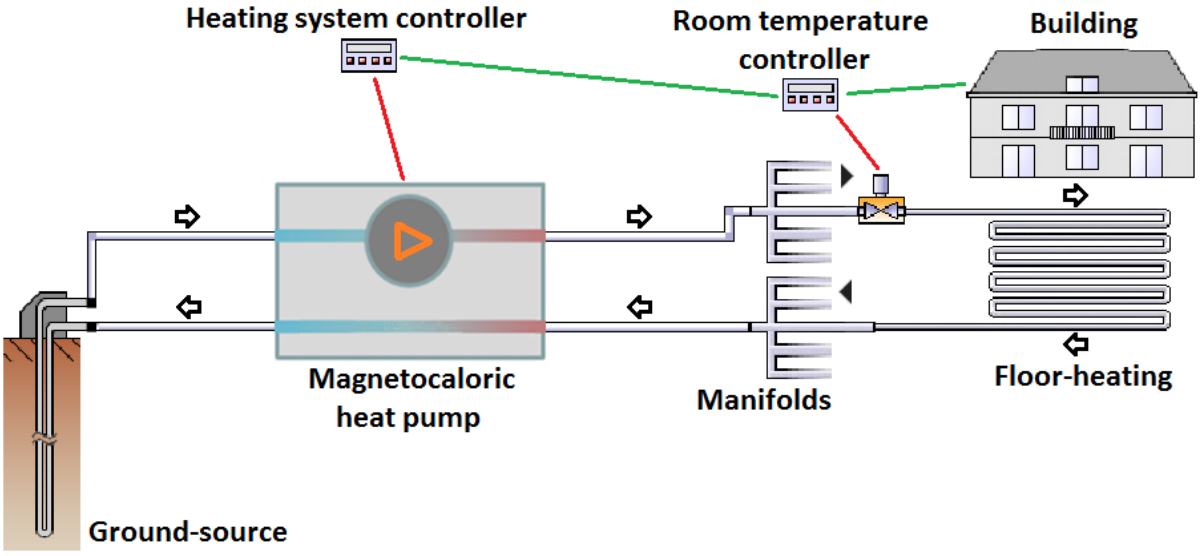

Figure 3: Integration of a magnetocaloric heat pump in a single hydronic loop with vertical borehole ground source heat exchanger and under-floor heating system.

4.2 Cascading of magnetocaloric heat pumps

The inability to generate large temperature span between the heat source and the heat sink is a primary limitation of the current MCHP technology for building heating applications. As shown by Johra et al., (2018), a Gadolinium MCHP connected to a VBGSHE can provide a fluid outlet temperature of up to 27.6 °C, which is sufficient to heat up to 22 °C a well-insulated house equipped with a low-temperature UFH system. However, this fluid outlet temperature is not sufficient for space heating of a poorly-insulated dwelling.

One possible solution to overcome this limitation and increase the outlet fluid temperature of MCHPs lies in establishing cold-to-cold and hot-to-hot connections of the AMRs inside a cascaded magnetocaloric heating network (Tahavori et al., 2017; Filonenko et al., 2018a; Filonenko et al., 2018b). Cascading has the potential for increasing the AMR temperature span ΔT_{AMR}, based on the principle explained in *Figure 4*. The hot (cold) outlet of the n^{th} magnetocaloric heat pump MCHP#n with temperature $T^{o(n)}_H$ (temperature $T^{o(n)}_C$) is connected to the hot (cold) inlet of the $(n+1)^{th}$ magnetocaloric heat pump MCHP#(n+1) with temperature $T^{i(n+1)}_H$ (temperature $T^{i(n+1)}_C$). Since it is expected that the MCHP will heat the hot fluid, $T^{i(n)}_H < T^{i(n+1)}_H$, and cool down the cold fluid, $T^{i(n)}_C > T^{i(n+1)}_C$, the hot (cold) fluid will be

heated up (cooled down) more and more as it progresses through the cascade. As a result, the temperature difference between the outlet and the inlet on both sides ($\Delta T_H = T^{o(N)}_H - T^{i(1)}_H$ and $\Delta T_C = T^{i(1)}_C - T^{o(N)}_C$) must increase with each added MCHP. This leads to an augmentation of the total temperature span according to the following equation:

$$\Delta T_{AMR} \equiv T^{o(N)}_H - T^{o(N)}_C = T^{i(1)}_H - T^{i(1)}_C + \Delta T_H + \Delta T_C \quad (3)$$

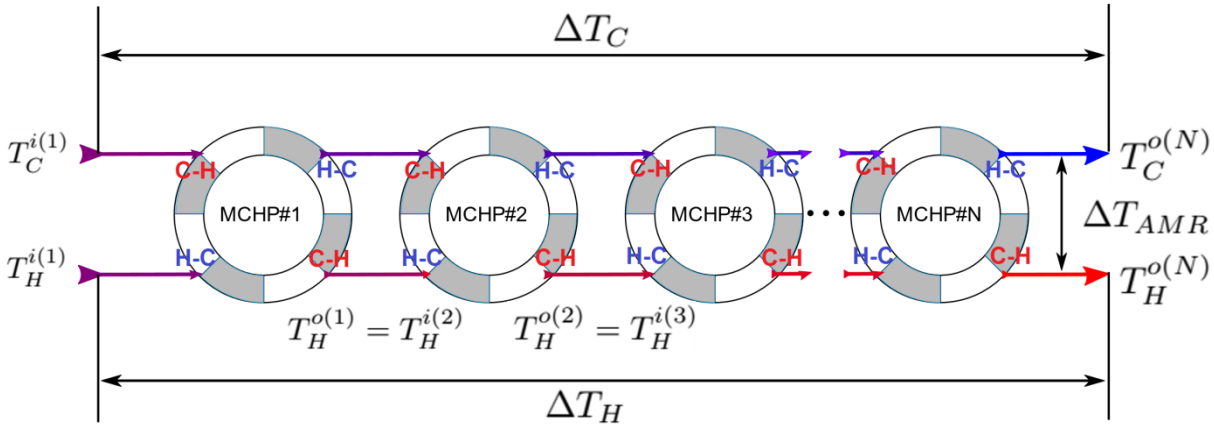

Figure 4: Cascading connection diagram (hot-to-hot and cold-to-cold rule).

Equation (3) defines the temperature span of the cascade as a difference between the hot and the cold outlet of the system, which coincide with the hot and the cold outlets of the last heat pump, MCHP#N. As one can see, the hot and cold temperature spans, ΔT_H and ΔT_C, are the main characteristics of the cascaded network, which relate its "outlet" and "inlet" temperature spans (ΔT_{AMR} and $T^{i(1)}_H - T^{i(1)}_C$).

The flows of fluid in and out of each heat pump during the hot-to-cold and the cold-to-hot blows are denoted in *Figure 4* by C-H and H-C, respectively. From a dynamic point of view, all hot-to-cold blows in the network occur simultaneously during a low field period accepting heat from the heat source at the cold end of the MCHP#1. In the same way, all cold-to-hot blows in the network occur simultaneously during the high-field period rejecting heat at the hot end of the MCHP#N. The coupling of the inlet and outlet temperatures of different heat pumps happens through Dirichlet boundary conditions imposed in individual MCHP models. It is important to keep in mind that because the boundary conditions are obtained under quasi-steady state approximation, the cascading model is an approximation. The latter should be verified in future work against fully transient simulations.

The magnetocaloric network properties established in previous studies (Filonenko et al., 2018a) give a way to simulate and compare the temperature span enhancement in various configurations of cascaded magnetocaloric heating networks (cascades). For simplicity, it is assumed that all MCHP blocks in *Figure 4* contain the same number of AMR beds N_{bed}. When comparing cascades with different number of MCHPs N_{MCHP}, the total MCM mass $m_T = m_{MCHP} \times N_{MCHP}$ of the network is kept constant, forcing a single heat pump mass m_{MCHP} to be inversely proportional to N_{MCHP}. Since the MCHP prototypes have almost identical AMRs, this mass can be found as $m_{MCHP} = m_{bed} \times N_{bed}$. The relationship between different scaling factors can, therefore, be written as:

$$N_{MCHP} \times N_{bed} = m_T/m_{bed} \quad (4)$$

It is required that N_{bed} and N_{MCHP} are both integers, therefore, the AMR mass cannot be chosen freely, but must be a divisor of the total cascade mass. In all simulations, m_T and m_{bed}

are both set constant according to a scaling factor $N_{MCHP} \times N_{bed} = 24$. A single MCHP consisting of 24 AMRs connected separately to a common heat source and a common heat load (parallel connection) is used as reference case. Several cascades are then constructed by grouping these AMRs inside several identical heat pumps without changing their total number or their individual properties, as illustrated in *Figure 5*. The connections between different heat pumps in each cascade correspond to the diagram in *Figure 4*. The detailed numerical model of the AMR system is firstly used to generate the output data for a single MCHP with cold side temperatures ranging from 0 °C to 15 °C, and hot side temperatures ranging from 20 °C to 40 °C. Lookup tables containing operation data are then generated and scaled to calculate the models for each of the heat pumps presented in *Figure 5*:

1. Single MCHP with $N_{bed} = 24$ AMRs connected in parallel ($N_{MCHP}=1$).
2. Two cascaded (hot-to-hot and cold-to-cold connected) MCHPs consisting of $N_{bed} = 12$ AMRs connected in parallel ($N_{MCHP}=2$).
3. Three cascaded MCHPs consisting of $N_{bed} = 8$ AMRs connected in parallel. ($N_{MCHP}=3$)
4. Four cascaded MCHPs consisting of $N_{bed} = 6$ AMRs connected in parallel ($N_{MCHP}=4$).
5. Six cascaded MCHPs consisting of $N_{bed} = 4$ AMRs connected in parallel ($N_{MCHP}=6$).
6. Eight cascaded MCHPs consisting of $N_{bed} = 3$ AMRs connected in parallel ($N_{MCHP}=8$).
7. Twelve cascaded MCHPs consisting of $N_{bed} = 2$ AMRs connected in parallel ($N_{MCHP}=12$).
8. Twenty-four cascaded MCHPs consisting of $N_{bed} = 1$ AMRs ($N_{MCHP}=24$). In this case it would not be practical to use the design described in previous sections, because the individual AMRs are cascaded, which is reflected in the *Figure 5*.

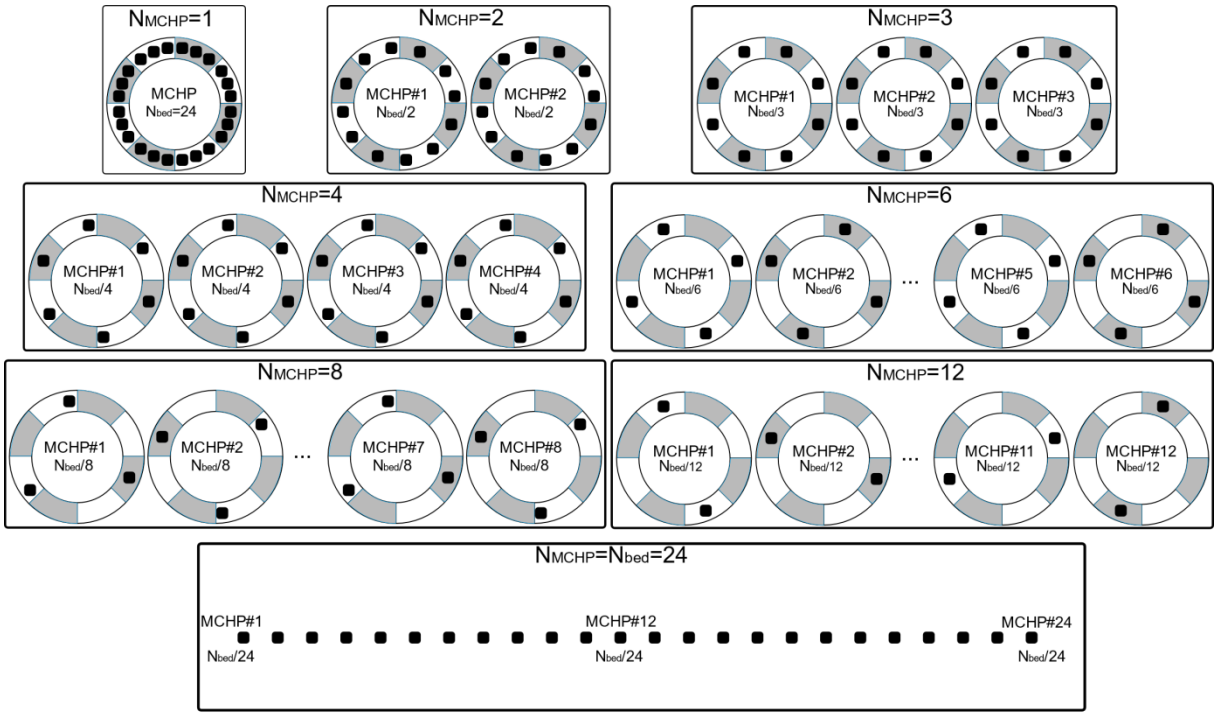

Figure 5: Cascade configurations produced by reconnecting the 24 regenerators of a single MCHP into identical MCHPs in all possible ways.

The cascading was implemented by equating the inlet temperatures of each next MCHP to the outlet of the previous, e.g. $T_o{}^{(n)}{}_H = T_i{}^{(n+1)}{}_H$. The cooling and heating powers were calculated as:

$$Q_C = \Sigma\, Q_{Cn,HP}(m_{MCHP}) = N_{bed}\,(Q_{C1} + Q_{C2} + \ldots + Q_{CN}) \quad (5)$$

$$Q_H = \Sigma\, Q_{Hn,HP}(m_{MCHP}) = N_{bed}\,(Q_{H1} + Q_{H2} + \ldots + Q_{HN}) \quad (6)$$

Eqations (5) and (6) assume that all of the cascaded heat pumps contain the same amount of AMRs connected in parallel. Q_{H1}, Q_{H2} , …, Q_{HN}, $Q_{Cn,HP}$ denote the heating powers of AMRs belonging to different heat pumps MCHP#1, MCHP#2, …, MCHP#N and the total n^{th} heat pumps power, respectively.

5. RESULTS

This section compares the results of numerical tests performed with different configurations of MCHPs and cascaded implementations. The 2 cascaded configurations have been selected among the aforementioned ones for their ability to deliver higher outlet fluid temperature:

- Single MCHP with Gadolinium as MCM.
- Single MCHP with $La(Fe,Mn,Si)_{13}H_y$ as MCM (layered regenerator).
- 12 cascaded MCHPs with Gadolinium as MCM comprising 2 AMRs each connected in parallel.
- 4 cascaded MCHPs with $La(Fe,Mn,Si)_{13}H_y$ as MCM comprising 6 AMRs each connected in parallel (layered regenerators).

All the results are calculated for a four-month test heating period (1^{st} of January to 30^{th} of April). Two coefficients of performance are used here to assess the MCHP efficiency: COP_{AMR} is calculated with the useful heating power delivered by the MCHP and only considering the work due to the AMR internal operation (regenerator hydraulic pressure losses and magnetic work); The COP_{system} is calculated with the useful heating power and considering all the work power usage of the heating system including circulation pump work, motor work and valves work (Johra et al., 2018). The rotation frequency of the MCHP system is always kept constant at 1 Hz.

5.1 Nominal performance tests of the magnetocaloric heat pumps

The initial numerical tests are performed with the MCHPs running at constant fluid flow rate and heating up only one thermal zone of the well-insulated house (living room) during the four-month heating test period.

One can see in *Figure 6* the useful heating power outputs of the different MCHP configurations. When the fluid flow rate is increasing, the power output of the MCHP is increasing almost linearly until a certain point. The higher the flow rate passing through each AMR and the more heat energy can be exchanged between the regenerator bed and the fluid. However, above an optimum point, further increase of the fluid flow rate disturbs the temperature profile of the AMR, causing a drop of the temperature output. Consequently, the MCHP heating power decreases rapidly (Li et al. 2006). In addition, higher fluid flow rate increases pumping work due to pressure losses in the hydraulic system, which decreases the system's COP even more. To improve the heating power output of the AMR system with higher fluid flow rates, the operational rotation frequency of the MCHP has to be increased, which brings other technical challenges.

With a maximum average heating power of 158 W, the Layered $La(Fe,Mn,Si)_{13}H_y$ single MCHP has a very limited power compared to the other configurations. The Gadolinium single MCHP presents a linear increase of its power output with a maximum average value of 2560 W at maximum fluid flow rate. The cascade systems present a heating power peak at 2935 W and 3652 W for the Gadolinium cascaded MCHPs and the Layered $La(Fe,Mn,Si)_{13}H_y$ cascaded MCHPs, respectively. However, one can notice that the maximum heating power output of the cascaded configurations occurs at lower fluid flow rate than the Gadolinium single MCHP, especially in the case of the Gadolinium cascaded MCHPs.

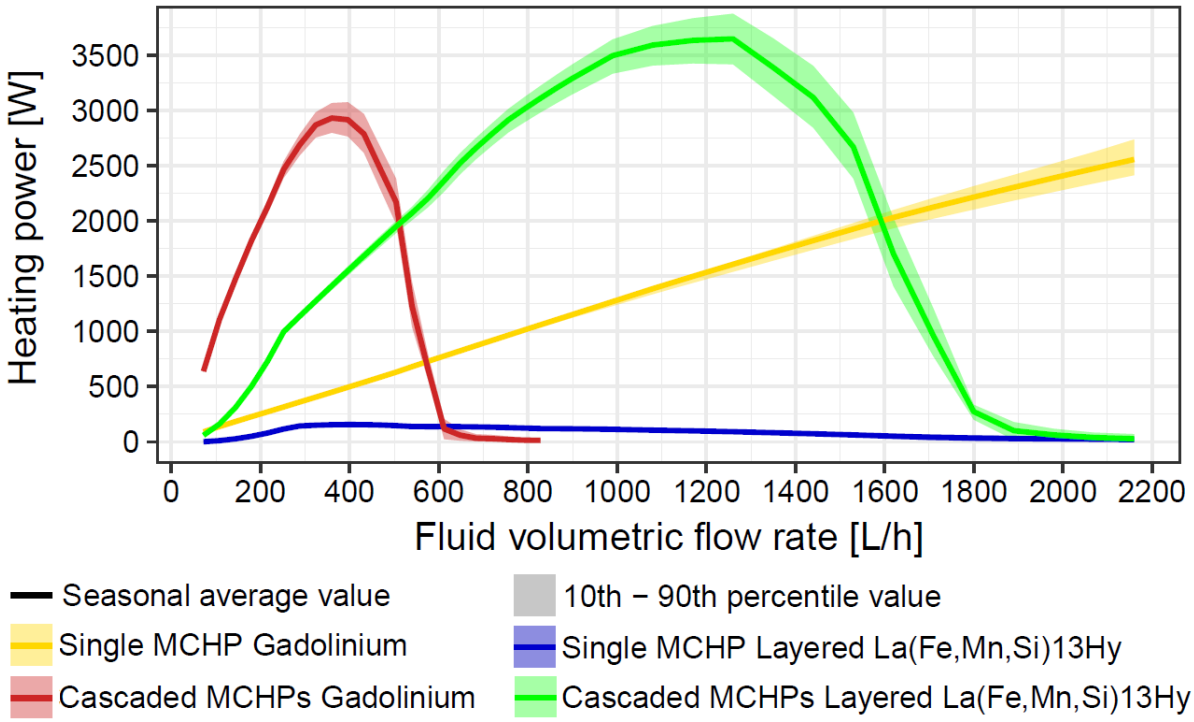

Figure 6: Heating power production of the MCHP as function of fluid volumetric flow rate.

Similar trends can be seen in *Figure 7* concerning the MCHP outlet fluid temperature. The maximum average outlet fluid temperature of the Layered $La(Fe,Mn,Si)_{13}H_y$ single MCHP is 22.3 °C (12 K temperature span), which is very critical for indoor space heating purpose. The other configurations manage to produce more appreciable fluid temperature outlet with a maximum average value of 27.6 °C (19.9 K temperature span), 35.3 °C (26.7 K temperature span) and 30.3 °C (23.8 K temperature span) for the Gadolinium single MCHP, the Gadolinium cascaded MCHPs and the Layered $La(Fe,Mn,Si)_{13}H_y$ cascaded MCHPs, respectively.

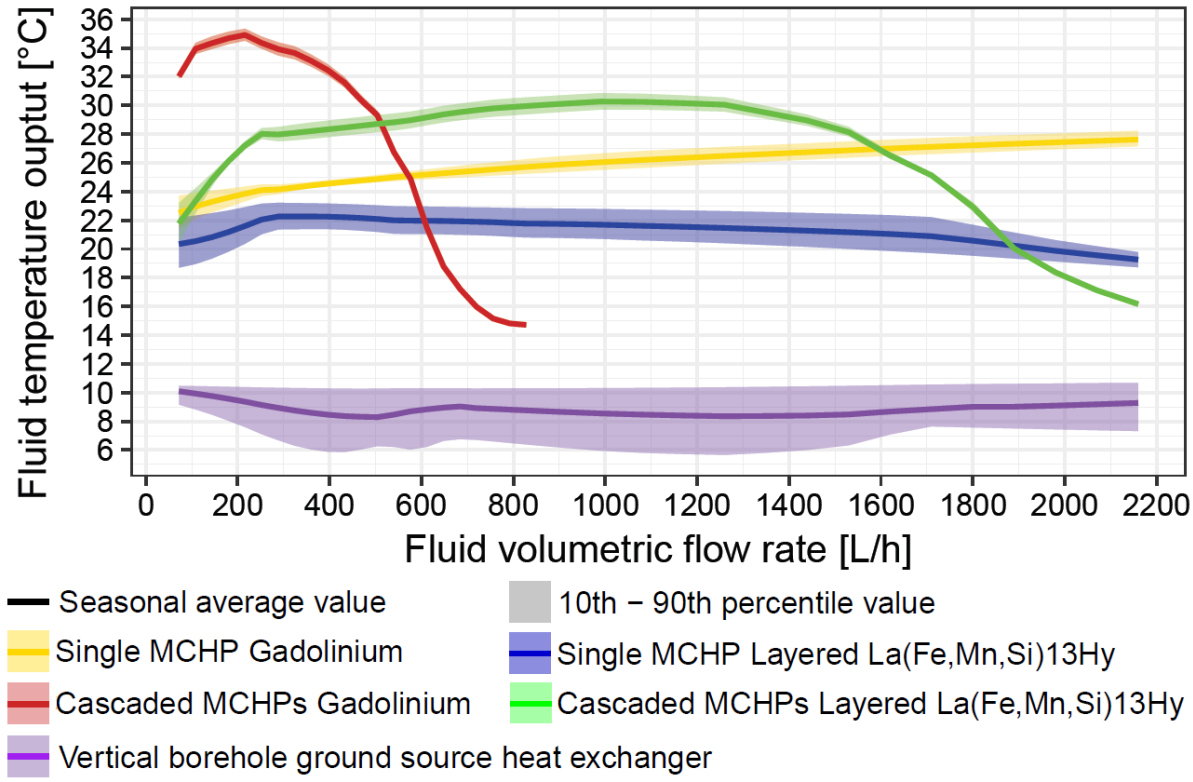

Figure 7: Fluid temperature output of the MCHP as function of fluid volumetric flow rate.

Concerning the systems energy efficiency, one can see in *Figure 8* that the COP_{AMR} (only considering the AMR internal operation efficiency) of the Gadolinium single MCHP, the Gadolinium cascaded MCHPs and the Layered $La(Fe,Mn,Si)_{13}H_y$ cascaded MCHPs reaches high values for low fluid flow rates. For these cases, the maximum average COP_{AMR} is 12.1, 6.9 and 12.3, respectively. Because the Layered $La(Fe,Mn,Si)_{13}H_y$ single MCHP has a much lower heating power output but has similar operational hydraulic pressure losses and magnetic work, its COP_{AMR} is much lower with a maximum average value of 3.3.

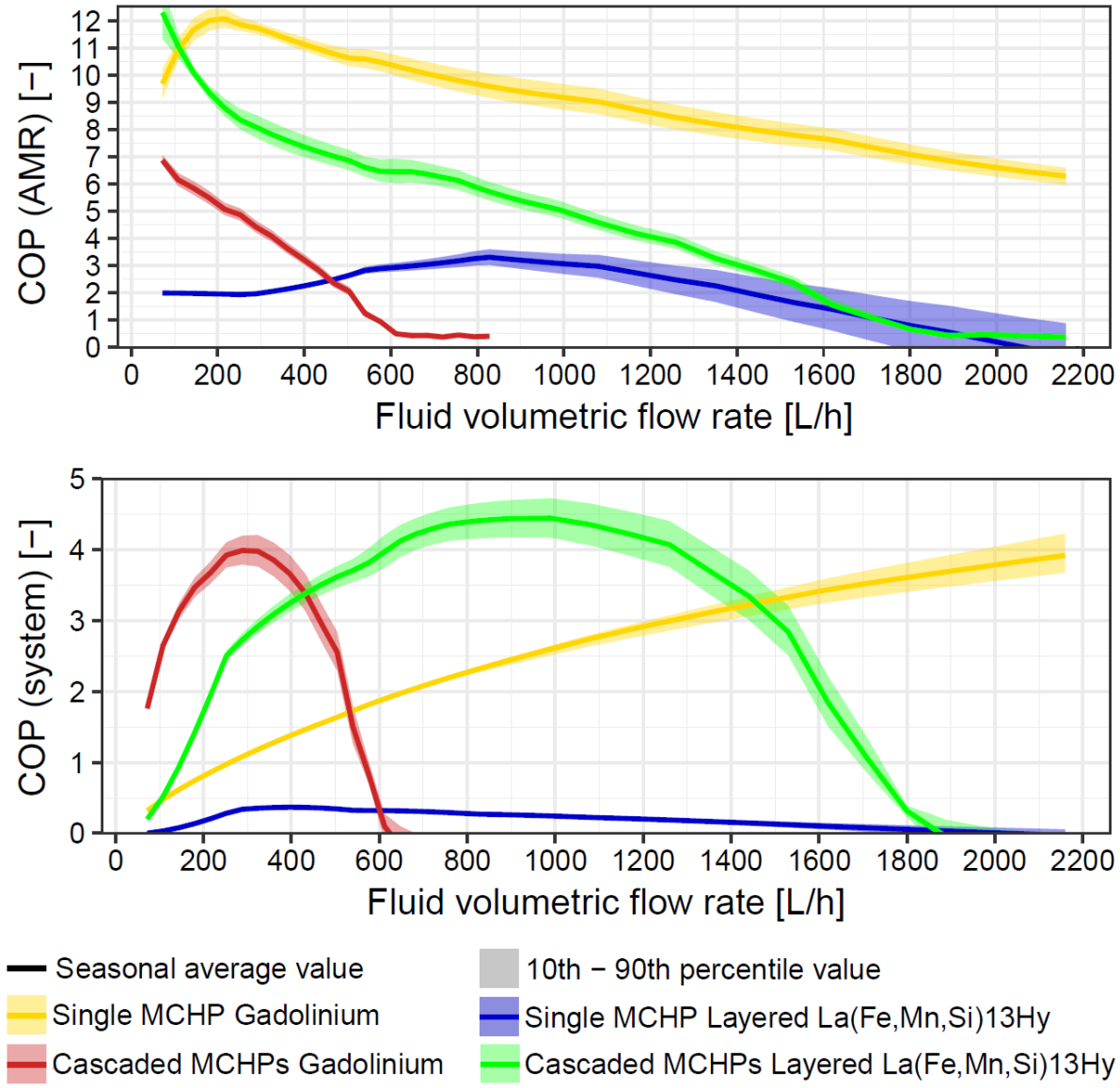

Figure 8: COP_{AMR} (top figure) and COP_{system} (bottom figure) of the MCHP as function of fluid volumetric flow rate.

The COP_{system} profiles of the different MCHP configurations is very similar to the heating power output curves because the work input needs of the entire heating system is rather stable over the whole range of fluid flow rates. The maximum average COP_{system} is 3.92, 0.37, 3.99 and 4.45 for the Gadolinium single MCHP, the Layered $La(Fe,Mn,Si)_{13}H_y$ single MCHP, the Gadolinium cascaded MCHPs and the Layered $La(Fe,Mn,Si)_{13}H_y$ cascaded MCHPs, respectively. One can observe that the Gadolinium single MCHP and the Layered cascaded MCHPs have very appreciable COP_{system} which are within the 3 - 5 range of typical COPs for conventional vapor-compression heat pumps (Self et al., 2013; Fischer and Madani, 2017). However, the significant difference between the COP_{AMR} and the COP_{system} indicates that a large part of the system's inefficiency is due to energy losses associated to the pump, the motor and the valves. The reduction of the latter constitutes a compelling engineering challenge for the development of this technology.

5.2 Test of a well-insulated house with a single MCHP

In this section, the 2 single MCHPs are tested numerically to provide for the indoor space heating needs of the entire building study case: a well-insulated single family house with a low-temperature UFH system. As shown previously, the Gadolinium single MCHP can provide enough heating power output to warm up the entire building. Therefore, only one of it is integrated in the well-insulated dwelling. On the other hand, the Layered La(Fe,Mn,Si)$_{13}$H$_y$ single MCHP has a very limited heating power output. Therefore in that case, one MCHP is integrated in each of the thermal zone UFH sub-circuits.

The controller of the Gadolinium MCHP is an ON/OFF controller connected to individual thermostats in each room of the house. Similarly, each of the Layered La(Fe,Mn,Si)$_{13}$H$_y$ MCHP is controlled with an ON/OFF controller connected to the thermostat of the corresponding thermal zone. In this case, the operational MCHP fluid flow rate is set to 400 L/h for optimum performance (according to previous section's tests).

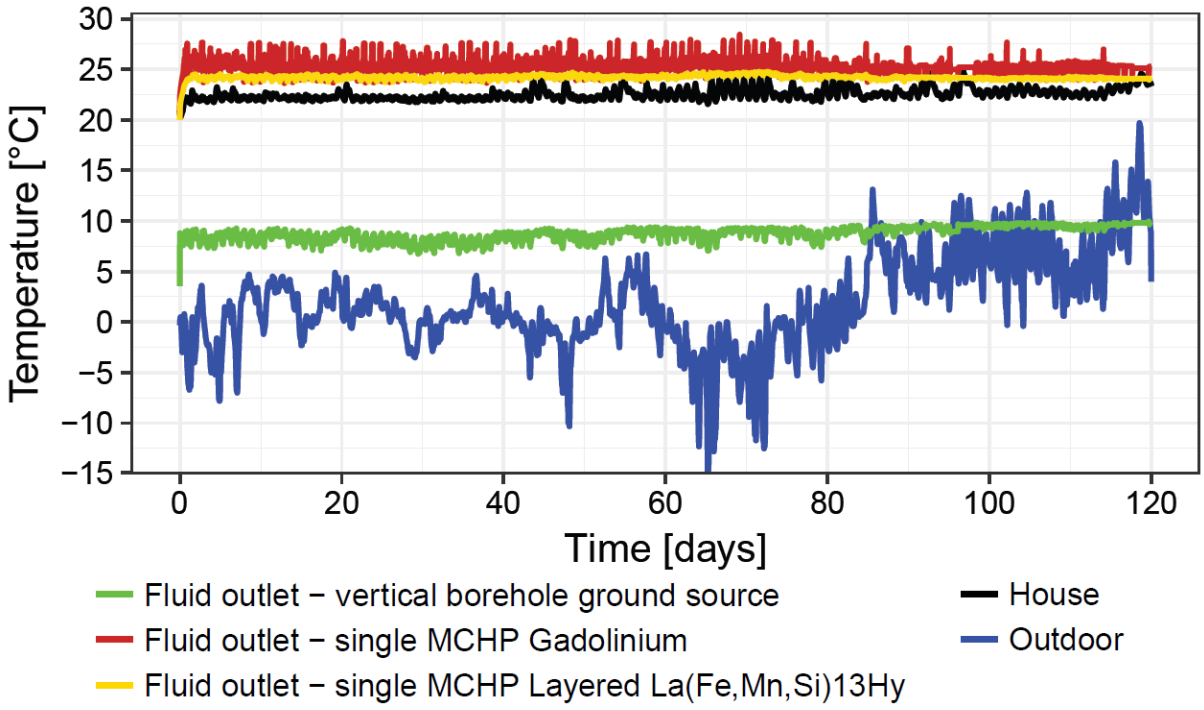

Figure 9: Temperatures of the building system as function of time during the four-month heating test period for the well-insulated house cases with single MCHPs.

Both the Gadolinium and the Layered La(Fe,Mn,Si)$_{13}$H$_y$ single MCHPs manage to provide enough heating power to keep the well-insulated house at an indoor temperature set point of 22 °C during the four-month heating test period. One can see in *Figure 9* that the Gadolinium system provides a higher fluid temperature outlet (25.4 °C in average) compared to the Layered La(Fe,Mn,Si)$_{13}$H$_y$ one (24.2 °C in average). The oscillations of fluid temperature in the hydronic systems are induced by the start-and-stop cycles of the MCHP.

However, one can clearly observe in *Figure 10* that the Gadolinium heating system has a much higher energy efficiency (average seasonal COP$_{system}$ of 1.84) compared to the Layered La(Fe,Mn,Si)$_{13}$H$_y$ one (average seasonal COP$_{system}$ of 0.57). In the full-house heating test, the COP of the Gadolinium system is much lower than the maximum COP achieved in the previous section's test. This is due to the fact that the controller of the Gadolinium single

MCHP does not manage to operate the heating system at optimum (maximum) fluid flow rate most of the time. On the other hand, the average seasonal COP of the Layered $La(Fe,Mn,Si)_{13}H_y$ system is higher than the maximum COP achieved in the previous section's test. This is because implementing one MCHP per UFH sub-loop induces a significant increase of the total heating power production while the pumping work (which holds a large share of the total system's inefficiency) remains relatively stable.

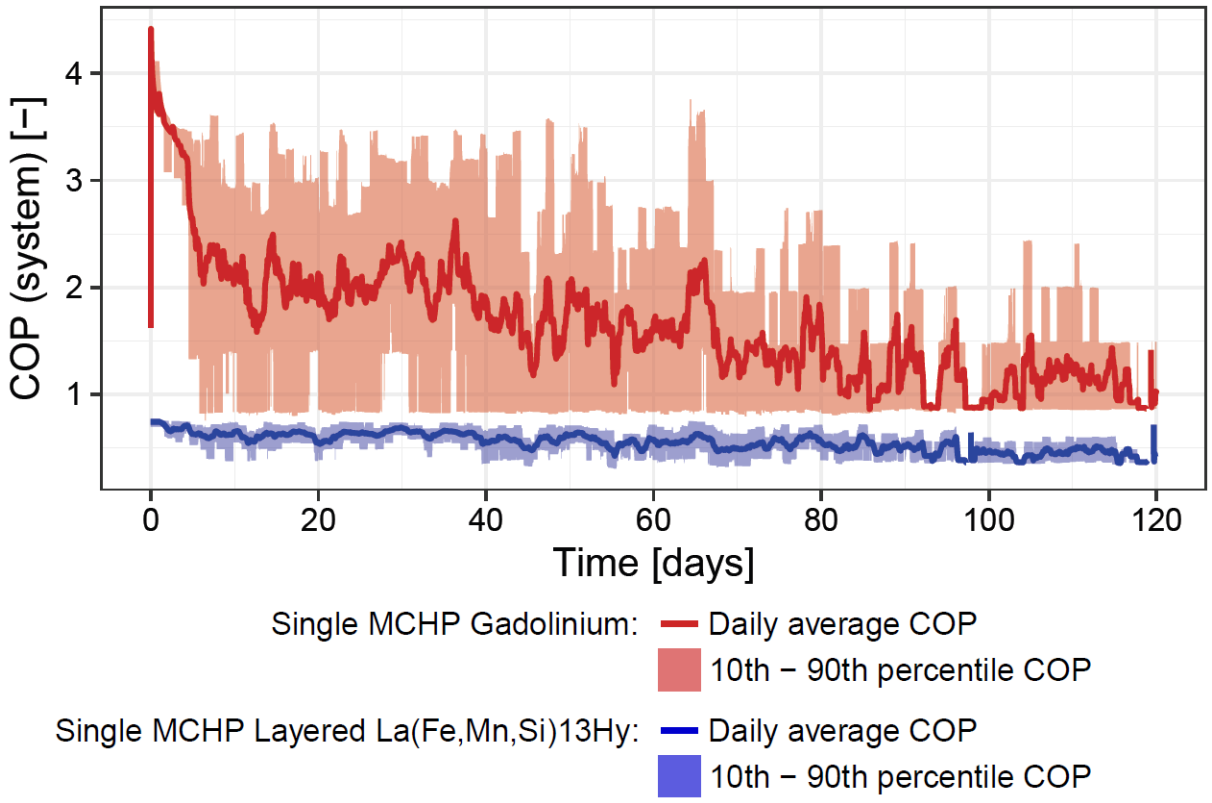

Figure 10: COP of the entire heating system as function of time during the four-month heating test period for the well-insulated house cases with single MCHPs.

5.3 Test of a poorly-insulated house with cascaded MCHPs

In this section, the 2 cascaded MCHPs systems are tested to provide for the indoor space heating needs of the entire building study case: a poorly-insulated single family house with a high-temperature UFH system. Because the envelope thermal performance of this building is lower than in the previous section's test, the usage of cascaded MCHPs systems is required to provide higher heating power output and warmer fluid inlet to each room in the house. Similarly to the Layered $La(Fe,Mn,Si)_{13}H_y$ single MCHP case, there is one cascaded MCHPs system integrated in each of the thermal zone UFH sub-circuits. It is therefore ensured that enough heating power is provided to all rooms in the dwelling.

For both cascaded heating systems, the MCHPs are controlled with an ON/OFF controller connected to the thermostat of the corresponding thermal zone. To ensure optimum performance (according to previous section's tests), the operational MCHP fluid flow rate is set to 300 L/h and 1000 L/h for the Gadolinium and the Layered $La(Fe,Mn,Si)_{13}H_y$ system, respectively.

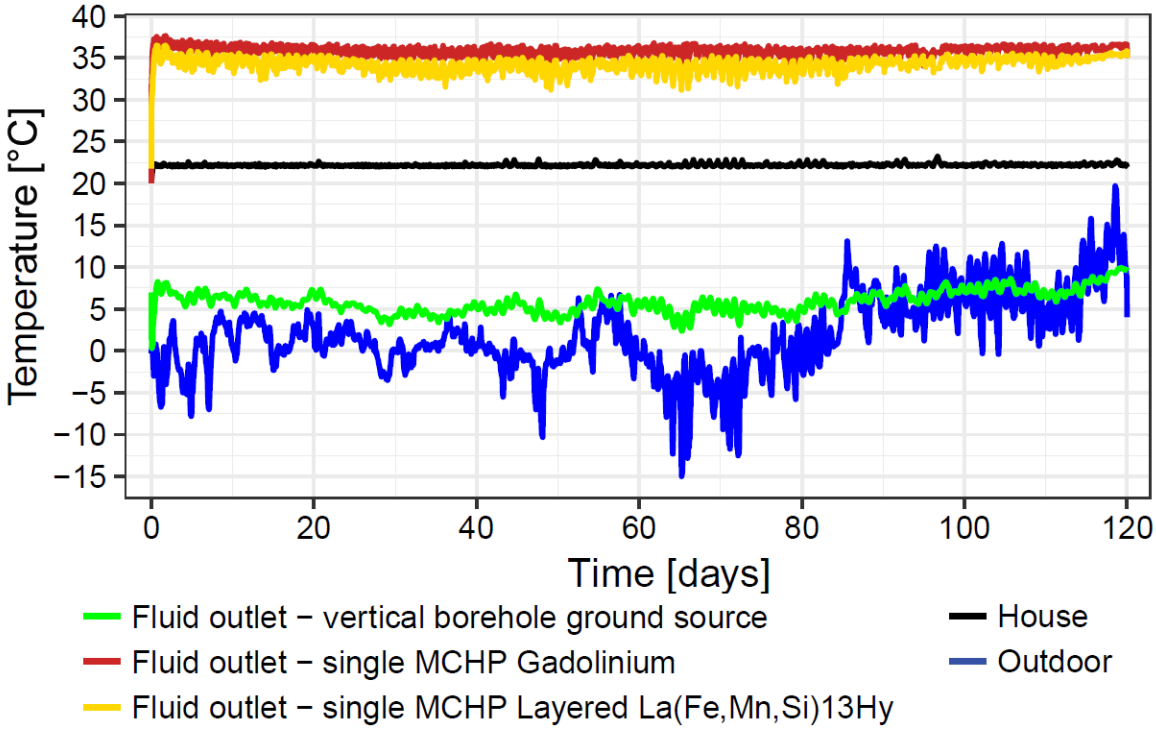

Figure 11: Temperatures of the building system as function of time during the four-month heating test period for the poorly-insulated house cases with cascaded MCHPs.

Both the Gadolinium and the Layered $La(Fe,Mn,Si)_{13}H_y$ cascaded MCHPs manage to provide enough heating power to keep the poorly-insulated house at an indoor temperature set point of 22 °C during the four-month heating test period. One can see in *Figure 11* that the Gadolinium system provides a higher fluid temperature outlet (36.0 °C in average) compared to the Layered $La(Fe,Mn,Si)_{13}H_y$ one (34.3 °C in average).

However, one can observe in *Figure 12* that both systems have an appreciable and very similar energy efficiency. The average seasonal COP_{system} is 2.62 and 2.63 for the cascaded MCHPs Gadolinium and the cascaded MCHPs Layered $La(Fe,Mn,Si)_{13}H_y$, respectively. This result is coherent with the previous nominal performance tests indicating that both cascaded systems have similar COP_{system} at optimum fluid flow rate.

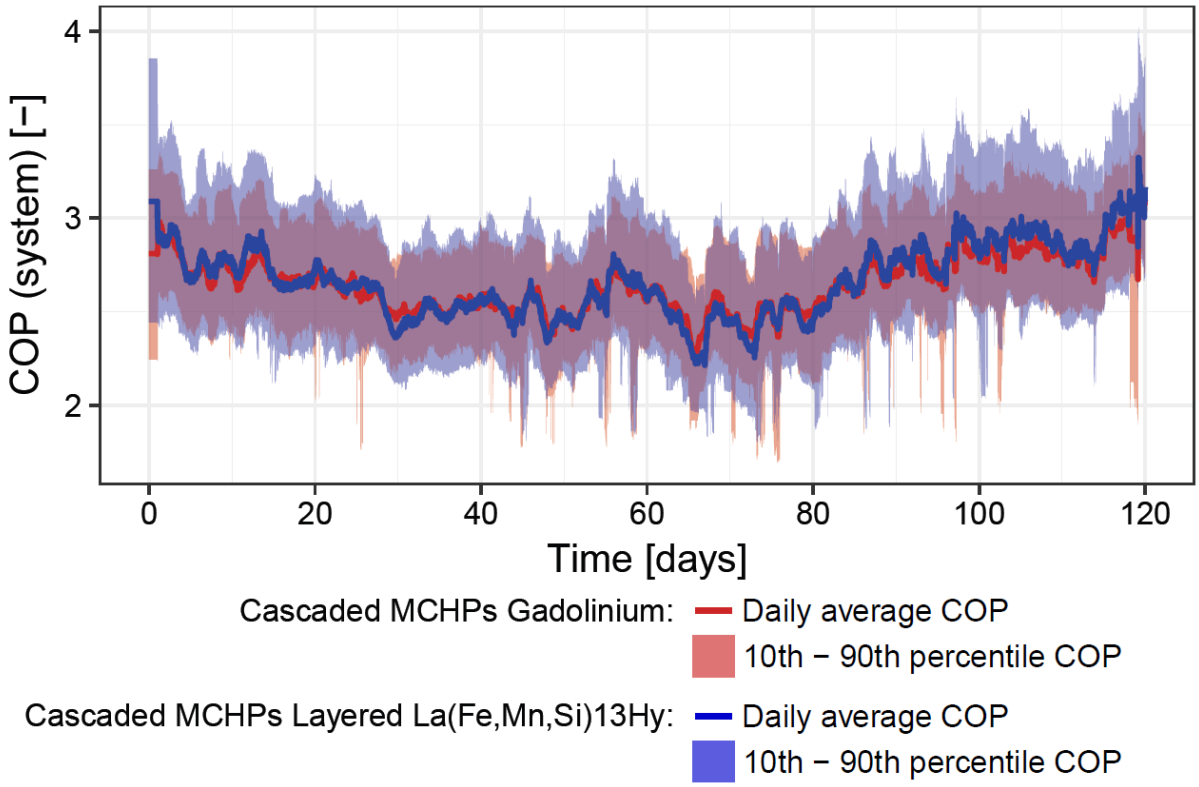

Figure 12: COP of the entire heating system as function of time during the four-month heating test period for the poorly-insulated house cases with cascaded MCHPs.

6. CONCLUSION

This article presented an innovative heat pump system based on the magnetocaloric effect and showed that it can be used for building heating applications. The active magnetic regenerator technology for magnetocaloric heat pump systems has the potential for high coefficient of performance but has yet to prove its competitiveness in comparison to vapor-compression devices. Currently, the main limitation of the magnetocaloric heat pump systems is the small temperature span they can generate between heat source and heat sink. To overcome this problem, the creation of cascaded magnetocaloric heating networks appears to be an interesting solution.

This numerical investigation has shown that different configurations of magnetocaloric heating system can provide enough heating power output for building applications. At nominal fluid flow rate, the magnetocaloric heat pumps could provide fluid temperature outlet at up to 35.3 °C and presents nominal coefficient of performance of up to 4.45.

When integrated in a single family house equipped with an under-floor heating system and a ground source heat exchanger, the magnetocaloric heating system was able to keep the dwelling at a set point temperature of 22 °C during the entire heating test period under Danish winter conditions. For well-insulated houses, single magnetocaloric heat pump systems were sufficient to operate with low-temperature under-floor heating systems. However, average seasonal COPs were not higher than 1.84. In the case of poorly-insulated houses, cascaded magnetocaloric heating networks were able to provide higher fluid temperature output to the under-floor heating system while operating at appreciable average seasonal COPs of up to 2.63.

Further research in the field of magnetocaloric technology is necessary to make the latter cost-effective and able to compete with conventional heat pump system. New magnetocaloric materials should be developed and characterized. More numerical and experimental test should be conducted on magnetic heating system and the different configurations of cascaded magnetocaloric heating networks.

ACKNOWLEDGEMENT

This work was financed by the ENOVHEAT project, which is funded by Innovation Fund Denmark (contract no 12-132673).

REFERENCES

Bahl, C.R.H., 2015. *ENOVHEAT project summary: development of efficient novel magnetocaloric heat pumps*. http://www.enovheat.dk/Research/ProjectSummary

Barclay, J.A., and Steyert, W.A., 1982. *US Patent US4332135*.

Building Performance Institute Europe (BPIE), 2011. *Europe's Buildings under the Microscope, Executive Summary 2011*.

Chen, F. C., Murphy, R. W., Mei, V. C., and Chen, G. L., 1992. *Thermodynamic Analysis of Four Magnetic Heat-Pump Cycles*. Journal of Engineering for Gas Turbines and Power, 114(4), 715-720.

Cockroft, J., and Kelly, N., 2006. *A comparative assessment of future heat and power sources for the UK domestic sector*. Energy Conversion and Management, 47, 2349-2360.

Engelbrecht, K. 2008. *A Numerical Model of an Active Magnetic Regenerator Refrigerator with Experimental Validation.* Ph.D. thesis, University of Wisconsin, Madison.

Engelbrecht, K., Eriksen, D., Bahl, C.R.H., Bjørk, R., Geyti, J., Lozano, J.A., Nielsen, K.K., Saxild, F., Smith, A., and Pryds, N., 2012. *Experimental results for a novel rotary active magnetic regenerator*. International Journal of Refrigeration 35, 1498-1505.

Filonenko, K., Johra, H., Dall'Olio, S., Engelbrecht, K., Heiselberg, P., Bahl, C., and Veje, C. T., 2018a. *Simulation of a magnetocaloric heating network*. Submitted to 8th International Conference on Magnetic Refrigeration at Room Temperature.

Filonenko, K., Lei, T., Veje, C., Engelbrecht, K., Johra, H., Heiselberg, P. K., and Bahl, C. R. H., 2018b. *Magnetocaloric heating modules for scalable and efficient heating*. Submitted to International Journal of Thermal Sciences.

Fischer, D., and Madani, H., 2017. *On heat pumps in smart grids: A review*. Renewable and Sustainable Energy Reviews, 70, 342-357.

Giauque, W.F., and MacDougall, D.P., 1935. *The production of temperatures below one degree absolute by adiabatic demagnetization of gadolinium sulfate*. Journal of the American Chemical Society 57, 1175-1185.

International Energy Agency (IEA), 2013. *Transition to Sustainable Buildings: Strategies and Opportunities to 2050*.

Jacobs, S., Auringer, J., Boeder, A., Chell, J., Komorowski, L., Leonard, J., Russek, S., and Zimm, C., 2014. *The performance of a large-scale rotary magnetic refrigerator*. International Journal of Refrigeration 37(1), 84-91.

Johra, H., Filonenko, K., Heiselberg, P., Veje, C., Lei, T., Dall'Olio, S., Engelbrecht, K., and Bahl, C., 2018. *Integration of a magnetocaloric heat pump in a low-energy residential building*. Building Simulation: An International Journal.

Johra, H., 2018. *Integration of a magnetocaloric heat pump in energy flexible buildings*. Ph.D. thesis, Aalborg University, Aalborg.

Kitanovski, A., Tušek, J., Tomc, U., Plaznik, U., Ožbolt, M., and Poredoš, A., 2015. *Magnetocaloric Energy Conversion: From Theory to Applications*. New York: Springer International Publisher, New York.

Lei, T., Engelbrecht, K., Nielsen, K. K., and Veje, C. T., 2017. *Study of the geometries of active magnetic regenerators for room temperature magnetocaloric refrigeration*. Applied Thermal Engineering, 111, 1232-1243.

Li, P., Gong, M., Yao, G., and Wu, J., 2006. *A practical model for analysis of active magnetic regenerative refrigerators for room temperature applications*, International Journal of Refrigeration, 29, 1259-1266.

Lund, H., Möller, B., Mathiesen, B. V., and Dyrelund, A., 2010. *The role of district heating in future renewable energy systems*. Energy, 35(3), 1381-90.

Navickaitė, K., Neves Bez, H., Lei, T., Barcza, A., Vieyra, H., Bahl, C.R.H., and Engelbrecht, K., 2018. *Experimental and numerical comparison of multi-layered La(Fe,Si,Mn)13Hy active magnetic regenerators*. International Journal of Refrigeration 86, 322-330.

Okamura, T., and Hirano, N., 2013. *Improvement of the performance of a room temperature magnetic refrigerator using Gd-alloy*. Journal of the Japan Society of Applied Electromagnetics and Mechanics 21 (1), 10-14.

Palzer, A., and Henning, H. M., 2014. *A comprehensive model for the German electricity and heat sector in a future energy system with a dominant contribution from renewable energy technologies – Part II: Results*. Renewable and Sustainable Energy Reviews, 30, 1019-1034.

Self, S. J., Reddy, B. V., and Rosen, M. A., 2013. *Geothermal heat pump systems: Status review and comparison with other heating options*. Applied Energy, 111, 341-348.

Smith, A., Bahl, C.R.H., Bjørk, R., Engelbrecht, K., Nielsen, K.K., and Pryds, N., 2012. *Materials challenges for high performance magnetocaloric refrigeration devices*. Advances Energy Materials 2, 1288-1318.

Tahavori, M., Filonenko, K., Veje, C. T., Lei, T., Engelbrecht, K., and Bahl, C., 2017. *A Cascading Model Of An Active Magnetic Regenerator System*. Proceedings of the 7th International Conference on Magnetic Refrigeration at Room Temperature, Turin, Italy, IIF/IIR, 248-251.

Weiss, P., and Piccard, A., 1918. *Sur un nouveau phénomène magnétocalorique*. Comptes Rendus Acad. Sci. (Paris) 166, 352-354.